Center for Sustainability and the Global Environment
NELSON INSTITUTE FOR ENVIRONMENTAL STUDIES
UNIVERSITY OF WISCONSIN–MADISON

Description of the approach, data and analytical methods used for the Farms Under Threat 2040 projections of future agricultural land conversion

Technical Report

May 31, 2022

By

Yanhua Xie and Tyler J. Lark

University of Wisconsin-Madison

Nelson Institute Center for Sustainability and the Global Environment

in partnership with

American Farmland Trust

and

Conservation Science Partners, Inc.

Recommended citation:

Xie and Lark. (2022). Description of the approach, data and analytical methods used for the Farms Under Threat 2040 projections of future agricultural land conversion. Technical Report. May 31, 2022. Center for Sustainability and the Global Environment, University of Wisconsin-Madison.

Note: An associated manuscript is in preparation for submission to a scientific journal

Table of Contents

1. Introduction 3

2. Methods 4

2.1. Projecting urban land demands 5

2.2. Creating development suitability layers 8

2.3. Development restriction layers 10

2.4. Creating development probability layers 12

2.5. UHD and LDR projections 13

2.5.1. Allocation of UHD development 13

2.5.2. Allocation of LDR development 14

3. Model validation 14

4. Results and discussion 15

4.1. Evaluation of BAU models 15

4.2. Spatial patterns of BAU projections 18

References 21

1. Introduction

This document describes the methods used to generate projections of future urban development in support of American Farmland Trust's Farms Under Threat (FUT) data series and assumes basic familiarity with past FUT research products and reports. The data developed for this analysis aim to project the conversion of land from agricultural uses (i.e., croplands, pastureland, rangeland, and woodland associated with farms) to Urban and Highly Developed (UHD) and Low-Density Residential (LDR) land uses by the year 2040, relative to a 2016 baseline. The key data layers produced and described are as follows:

- UHD suitability layer (0-1): the location's urban development potential
- 2040 BAU UHD allocation (0 or 1): The specific locations that are most likely to be converted to UHD under a Business-as-Usual development demand scenario
- 2040 BAU LDR allocation (0 or 1): The specific locations that are most likely to be converted to LDR under a Business-as-Usual development demand scenario
- 2040 BBC UHD allocation (0 or 1): The specific locations that are most likely to be converted to UHD under a Best-Built-Cities development demand scenario
- 2040 BBC LDR allocation (0 or 1): The specific locations that are most likely to be converted to LDR under a Best-Built-Cities development demand scenario
- 2040 RS UHD allocation (0 or 1): The specific locations that are most likely to be converted to UHD under a Runaway-Sprawl development demand scenario
- 2040 RS LDR allocation (0 or 1): The specific locations that are most likely to be converted to LDR under a Runaway-Sprawl development demand scenario
- 2040 FP UHD allocation (0 or 1): The specific locations that are most likely to be converted to UHD under a Farmland-Protection development demand scenario
- 2040 FP LDR allocation (0 or 1): The specific locations that are most likely to be converted to LDR under a Farmland-Protection development demand scenario
- FP layer (0 or 1): The specific locations of farmland parcels to be protected

In this technical report, we focus mainly on the methods and validation for the Business-as-Usual (BAU) scenario, as it provides the baseline approach for all scenarios and results.

2. Methods

We assumed that a non-urban location being converted to urban land use is a function of the location's urban development potential (development suitability), development restrictions (e.g. protected or reserved for non-urban purposes), historical conversion rate (transition probability), and urban land demand (land increase for urban uses) (Chen et al. 2020; Seto et al. 2012). We specifically modeled two types of threats to agricultural land use: urban and highly developed (UHD) and low-density residential (LDR) land uses. These definitions were adopted from the Farmland Under Threat (FUT) layers created by American Farmland Trust (AFT) and Conservation Science Partners (CSP) (Freedgood et al. 2020; Sorensen et al. 2018). In general, UHD reflects developed lands classified as open spaces and low- to high-intensity urban land uses in USGS's National Land Cover Database (NLCD), whereas LDR refers to non-urban lands within U.S. Census Blocks with average acres-per-housing-unit smaller than approximately the 10th percentile of the farm size distribution for each county. In these low-density residential areas, we assume that agricultural lands that remain are under threat due to their proximity to residential areas, as the options for agricultural production may be increasingly limited or they could be further developed unless restrictive zoning or permanent protection is applied. For more information on the definitions of UHD and LDR, the processes for classifying them, and the reasoning behind such delineations, see the previous FUT technical report (https://s30428.pcdn.co/wp-content/uploads/sites/2/2021/06/AFT_CSP_FUT_Technical_Doc_2020.pdf).

Using this land classification framework, AFT identified and documented locations where conversion to UHD and LDR occurred from 2001 to 2016 (Freedgood et al. 2020). In this report, we projected continued conversion to UHD and LDR land uses between 2016 and 2040. In general, there are four steps involved in our projection process: (1) estimating demand for new UHD and LDR lands between 2016 and 2040, (2) creating suitability layers, (3) generating probability layers, and (4) conducting spatial allocation (Figure 1). We modeled UHD and LDR development under four different scenarios: Business-as-Usual (BAU), Runaway-Sprawl (RS), Better-Built-Cities (BBC), and Farmland Protection (FP). Except for the FP scenario that was conducted for ten select metropolitan areas, all other scenarios were modeled for the entire contiguous U.S. See SCENARIOS section of AFT's report, Farms Under Threat 2040: Choosing an Abundant Future, for more information about scenario design. We implemented all models at the level of counties at a spatial resolution of 30 meters on Google Earth Engine (GEE).

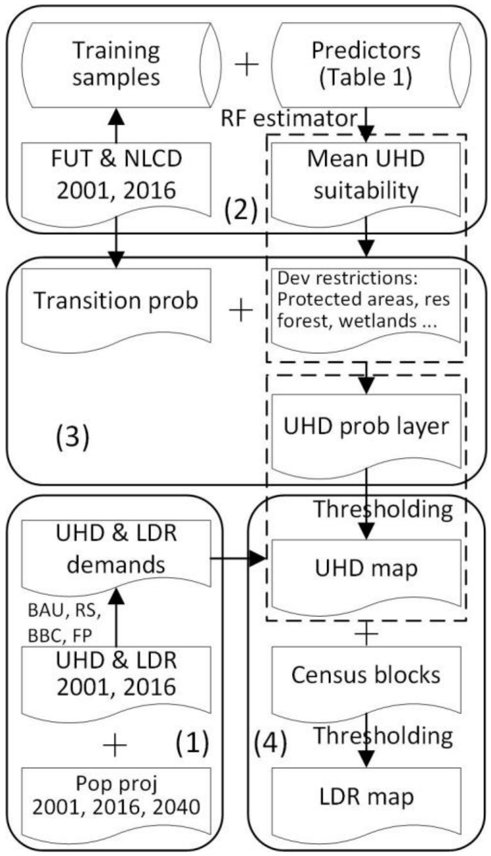

Figure 1. Framework of the modeling methods. (1) projecting demands, (2) calculating development suitability, (3) creating urban development probability, and (4) generating binary UHD and LDR projections. UHD: urban and highly developed; LDR: low-density residential.

2.1. Projecting urban land demands

In the BAU scenario, development remains on the same trajectory as that from 2001-2016, as documented in Farms Under Threat: The State of the States (Freedgood et al. 2020), driven by existing land-use policies and consumer preferences. For each county, we estimated UHD demand in 2040 ($devDemand_{uhd}$) as:

$$devDemand_{uhd} = uhdIncRate_{2001-2016} * 24 * adjFactor \tag{1}$$

where $uhdIncRate_{2001\text{-}2016}$ is the average annual UHD increase of a county from 2001 to 2016 (i.e., total UHD increment divided by 15), *adjFactor* is the state-level adjusting factor that is used for all counties within a state, and the number 24 refers to the number of years between 2016 and 2040. We used a population change-driven adjusting factor to reflect possible variations in urban development trajectories because 1) population increase is a good indicator of high-density urban development (e.g., more buildings are needed to house growing population) (Left inset of Figure 2), and 2) other indicators like gross domestic product (GDP) are not available at the scales needed. The adjusting factor was calculated as:

$$adjFactor = 1 + r * 0.1 \tag{2}$$

where *r* is the relative change rate of population growth between 2016-2040 and 2001-2016:

$$r = (popIncRate_{2016-2040} - popIncRate_{2001-2016})/abs(popIncRate_{2001-2016}) \tag{3}$$

where *popIncRate* is the average annual population increase (i.e., total population growth during a period divided by the number of years). Population estimates for the years 2001 and 2016 were from U.S. Census Bureau (https://www.census.gov/data/tables/time-series/demo/popest/intercensal-2000-2010-state.html and https://www.census.gov/data/tables/time-series/demo/popest/2010s-state-total.html), and the state-level population projections are from Weldon Cooper Center for Public Service, University of Virginia (see details here: https://demographics.coopercenter.org/national-population-projections/). Note that both projections consider domestic and international population migrations, but it is unclear whether and to what extent these predictions specifically include climate change-induced migration. However, because both datasets use the population census as reference, we assumed the estimates and projections are consistent and compatible across states and time.

The adjusting factor is calibrated by state given the lack of county-level population projections. This procedure of UHD demand estimation reflects the projected change in population growth rate, but it is also designed to not substantially over- or under-estimate future UHD needs. For example, if a state is projected to see 50% faster population growth in 2016-2040 than it did in 2001-2016, the UHD conversion rate would increase by 5%. As a result, the adjustment factor ranges from 0.8 to 1.1 for all states except for West Virginia, which has the largest projected decline in population growth rate (adjustment factor is 0.54).

Because LDR is usually near existing UHD, it is more likely to be urbanized than non-LDR land uses. We thus divided UHD demand into two components – LDR-to-UHD and non-LDR-to-UHD, so that future UHD development would occur on LDR at an appropriate rate. Assuming that the proportion of UHD development on LDR (compared to the total UHD development) remains unchanged from 2001-2016 to 2016-2040, the amount of future LDR-to-UHD conversion was estimated as:

$$devDemand_{ldr2uhd} = devDemand_{uhd} * prop_{ldr2uhd} \tag{4}$$

where $prop_{ldr2uhd}$ is the proportion of UHD development on LDR from 2001 to 2016. Subsequently, the amount of non-LDR-to-UHD conversion was calculated as $devDemand_{uhd} – devDemand_{ldr2uhd}$.

We used a similar method to estimate future LDR demand per county as:

$$devDemand_{ldr} = ldrIncRate_{2001-2016} * 24 \tag{1}$$

where $ldrIncRate_{2001-2016}$ is the average annual LDR increase of a county from 2001 to 2016 (i.e., total LDR increment divided by 15). However, we did not apply a population-driven adjusting factor for LDR demand estimation because LDR increases were found to have a weak relationship with population change (Right inset of Figure 2). Other important variables like farm distribution and farm size in 2040 were not available at the time of conducting this research.

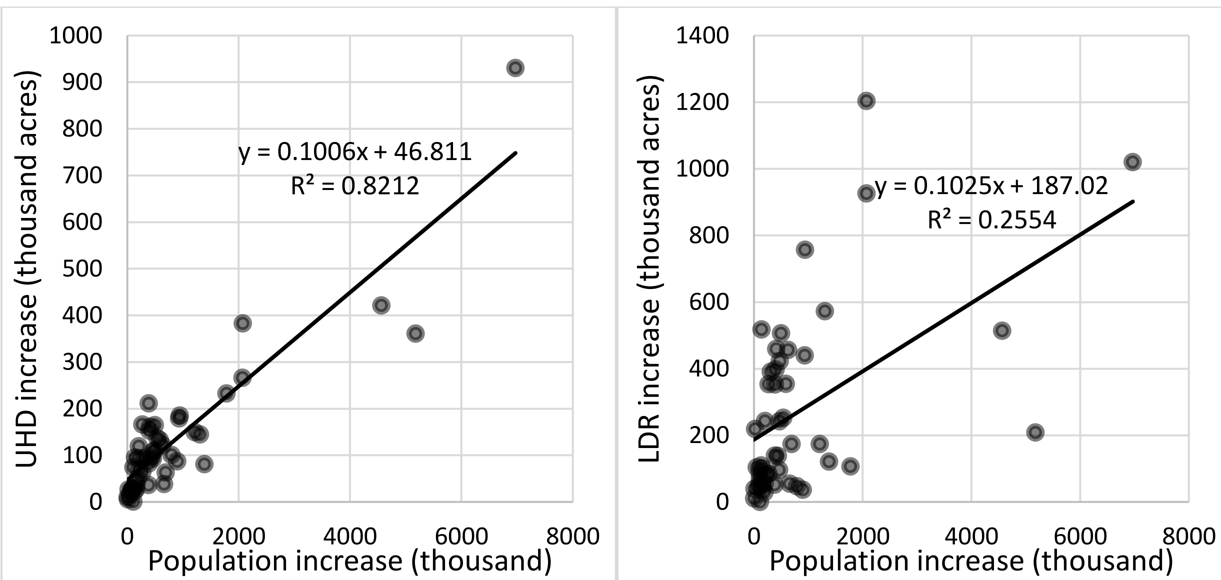

Figure 2. State-level relationships between population growth and urban area increases during 2001-2016 (Left: urban and highly developed; Right: low-density residential).

By using BAU estimation as the reference, we then estimated UHD and LDR demands for each scenario proportionally based on the conditions in Table 1. For the RS scenario, we kept UHD demand the same as in the BAU but increased LDR demand by 50%. For the BBC and FP scenarios, we reduced UHD and LDR demand by 25% and 50%, respectively. See SCENARIOS section of AFT's Report for more information about rationales for these settings.

Table 1. Modeling assumptions for the four scenarios.

Scenario	Rate of UHD conversion	Rate of LDR conversion	Farmland protection
Business as Usual	Historical rate, adjusted for future population growth	Historical rate	No new farmland protection
Runaway-Sprawl	Same as BAU	50% more than BAU	No new farmland protection
Better-Built-Cities	25% less than BAU	50% less than BAU	No new farmland protection
Farmland-Protection	25% less than BAU	50% less than BAU	New protection applied to 10% of agricultural lands in each metropolitan area

2.2. Creating development suitability layers

We estimated development suitability for each pixel within a county on a scale of 0 to 1 (higher values imply more suitable for development), with the potential for a location to be urbanized defined by a set of spatial and socioeconomic determinants (Table 2). Predictor variables included terrain, relationships to existing urban areas, transportation networks, water resources, other land resources (e.g., protected natural resources), urban fraction within a pre-defined buffer, land value, and nighttime light intensity (to account for scale-dependent effects of urban development, e.g., urban development can be more likely to occur around large cities for some counties).

We built the UHD suitability layer from these estimators by employing random forest classifiers (Breiman 2001). We did not create a specific LDR suitability layer because: (1) LDR is defined by farm size data that is not available for the year 2040 and (2) LDR has a high probability to be converted to UHD (i.e., UHD suitability is a strong indicator for LDR development). The computation of suitability layers was conducted per county. For each county, UHD and non-UHD training samples were randomly stratified from FUT and NLCD 2016 layers. We tested a series of sample sizes (from 50 to 1000 for each class with the increment of 50) for classifier training. While too dense of a sampling scheme can result in a problem of over-fitting the model, too few samples can exaggerate projections. After testing, we found reasonable results (based on visual inspection) were achieved using 400 samples (200 for each class) per county. County-specific random forest classifiers trained from stratified samples and predictor variables were then used to calculate UHD suitability layers. For counties with small UHD area in 2016 (i.e., smaller than 2 km^2), state-level classifiers were trained and applied with 2,000 samples for each class. The county-level suitability layers were then mosaicked to create a nationwide map.

As sample size and location is critical to image classification as well as to estimate suitability in this study, we repeated the procedure of sample stratification and suitability calculation 100 times. As a result, we created 100 nationwide suitability layers, which were then averaged to generate the mean suitability layer (see Figure 3 for an overview of UHD suitability). This final suitability layer was later used in the next steps of estimating development probability and spatial allocation

Table 2. Socioeconomic and physical variables used to estimate urban development suitability.

Variable name	Abbreviation	Spatial resolution	Year of data	Data sources
Nighttime light intensity	ntl	500 m	2016	NOAA NPP/VIIRS
Land value	landVal	480 m	2010	Nolte (2020)
Elevation	elevation	30 m	2000	NASS Shuttle Radar Topography Mission
Slope	slope	30 m	2000	
Distance to existing urban boundary	dist2urBound	30 m	2016	FUT2016 and NLCD2016
Distance to primary roads	dist2priRd	30 m	2016	TIGER: US Census Roads
Distance to secondary roads	dist2secRd	30 m	2016	
Distance to water bodies	dist2water	30 m	2016	NLCD2016
Size of the closest urban cluster	urSize	30m	2016	FUT2016

Urban fraction within a 1 km * 1km buffer	urRatio	1 km	2016	NLCD2016
Distance to forest	dist2forest	30 m	2016	NLCD2016
Distance to protected ag land	dist2Pal	30 m	2016	AFT PALD
Distance to protected areas	dist2pad	30 m	2019	PAD-US

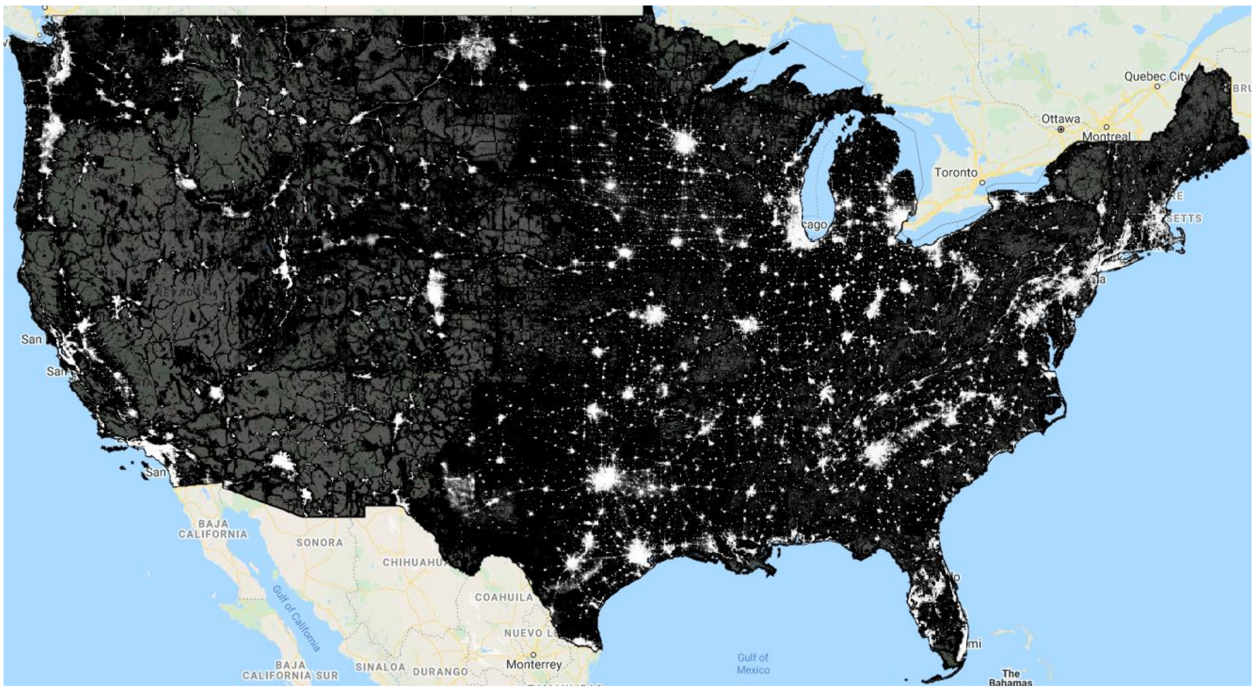

Figure 3. Overview of UHD suitability (black to white pixels represent low to high values; gaps occur where suitability is zero).

2.3. Development restriction layers

Certain land uses are assumed unlikely to be urbanized. These areas were removed from the suitability layer before conducting spatial allocation. In this study, development restrictions included existing UHD, federal lands, protected agricultural lands, Protected Areas Database of the U.S. (USGS PAD-US v.2.1), wetlands (only for UHD allocation), and water bodies. The extent of UHD, federal lands, wetlands, and water bodies were derived from FUT and NLCD 2016, and protected agricultural lands dataset (PALD) and PAD-US were from AFT and USGS, respectively.

In addition to these areas, forestlands within residential areas tend to remain unchanged given their importance to the living environment (e.g., reduced urban heat island, ecological and aesthetic values, etc.) (Nowak et al. 2008; Tyrväinen et al. 2003; Ziter et al. 2019) (Figure 4). However, residential forestlands are usually classified as LDR in FUT layers and are close to UHD, making them likely to receive high suitability values. To reserve these LDR areas, we developed a set of rules to identify them using random forest classifier. We first calculated the proportion of each US Census Block that was in LDR and other land cover/use classes (derived from FUT and NLCD layers). We then calculated maximum vegetation greenness in each Census Block for the years 2001 and 2016. To calculate vegetation greenness of a block, we first computed a layer of yearly maximum NDVI from all available Landsat images within a year (i.e., 2001 and 2016), which was then aggregated as the mean value of all pixels within the block. Blocks with and without LDR-to-UHD conversion during the period of 2001-2016 were then marked and used as reference to train state-wise random forest classifiers. Predictors included land use types and densities and vegetation greenness of the year 2001. The trained classifiers were later applied to 2016 predictors to predict LDR blocks likely to remain stable from 2016 to 2040. The detected stable LDR blocks were subsequently used as an additional restriction layer for 2040 UHD projection in a similar manner to the layers of protected agricultural lands and existing UHD extent.

For the FP scenario, we also projected future agricultural lands most likely to be protected and used these areas as an additional restriction layer. We purposely protected 10 percent of the most productive agricultural lands within each city/metropolitan area that are near existing agricultural land parcels under protection to represent the organizational goal of AFT. We assumed that highly important agricultural lands close to existing protected ones are more likely to be protected from future urbanization. For our proximity measure, we used an inverse distance weighting strategy and constrained this limit to 3 miles, such that the proximity value was set to 0 if a land parcel is beyond 3 miles of an existing protected one. Land importance was represented by the productivity, versatility, and resiliency (PVR) value, which is a combination of soil suitability, crop type and growing season length, and land cover/use type (see AFT PVR report for more details). Proximity and PVR were then integrated using the weights 0.2 and 0.8, respectively, as determined by a panel of experts ($0.2 \times$ proximity $+ 0.8 \times$PVR). Finally, a series of thresholds were applied to the integrated indicator until the 10 percent protection area was achieved. Note this analysis was conducted at the land parcel level derived from Loveland Parcel Dataset (https://regrid.com/parcels).

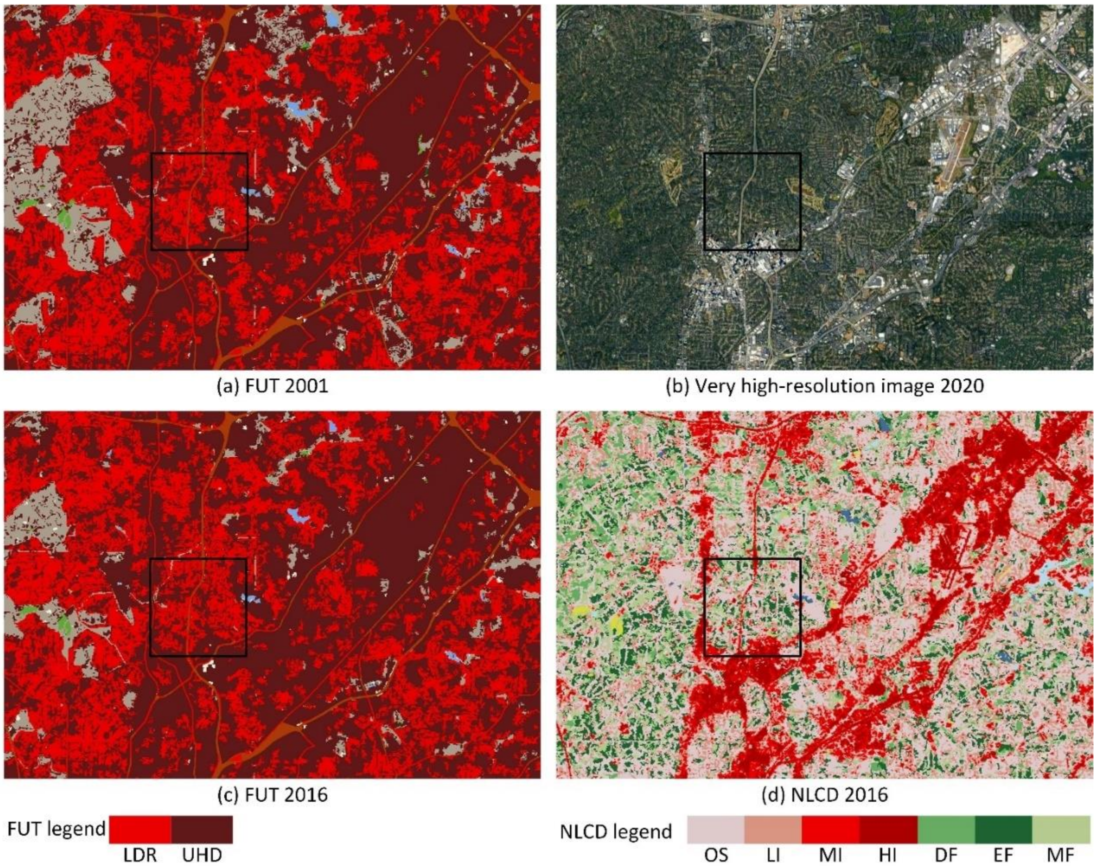

Figure 4. Residential forestlands northeast of Atlanta (highlighted in black rectangle, classified as LDR in FUT layers) that tend to remain unchanged in UHD development. OS: developed, open space, LI: developed, low intensity, MI: developed, medium intensity, HI: developed, high intensity, DF: deciduous forest, EF: evergreen forest, MF: mixed forest.

2.4. Creating development probability layers

Development probability is defined as the product of suitability and historical land use conversion rate (transition probability). We calculated the transition probability statistics at the county level based upon the actual conversion rate of each non-urban land use to urban use between 2001 and 2016 using FUT and NLCD layers. For each county, we calculated the amount of conversion to UHD of each land use in proportion to its total area from 2001 to 2016, including LDR, cultivated lands, forest, herbaceous, wetlands, bare land, and water bodies. Because LDR is an integrated class that covers all other land uses except for UHD, we further calculated transition probability of each land use within LDR.

The calculation of transition probabilities for each county was conducted only within the peri- to urban areas as defined by nighttime light brightness greater than 1. The reasons for this design are twofold. First, area of land uses can vary substantially within a county (e.g., some midwestern counties are dominated by croplands), which would lead to extremely higher or low transition probability if all land uses within the target county are counted. In fact, land uses remote from urban areas tend to remain unurbanized and should have low transition probability. Second, artificial nighttime lights were used to delineate urban and peri-urban boundaries because they have high correlations with human activities including urban extent (Elvidge et al. 1997; Sutton et al. 2007; Xie et al. 2019). The brightness threshold of 1 was used to cover the majority of 2016 LDR and UHD extent and remove possible background noise (i.e., small brightness for unlit areas due to systematic errors).

2.5. UHD and LDR projections

We projected the location of future UHD development using a pixel-based thresholding method. The projections of LDR-to-UHD and non-LDR-to-UHD were conducted separately due to the unique characteristics of LDR compared to other non-LDR land uses. After UHD allocation, the location of LDR development was estimated using a block-based thresholding method to maintain consistency with previous FUT approached and datasets. For each scenario, UHD and LDR development were assigned according to the associated level of urban demand. All projections were county-stratified and subsequently mosaiced to nationwide maps.

2.5.1. Allocation of UHD development

To estimate where LDR will be converted to UHD development, a county-stratified, pixel-based thresholding method was applied. After removing development restriction areas (Section 2.3) from the probability layer (Section 2.4), spatial allocation was applied based on pixel values and urban development demand from LDR (Section 2.1), i.e., locations with higher probability values are urbanized earlier than low value pixels. A series of thresholds (from 0 to 1 with step of 0.002) were used to segment the probability layer until the amount of LDR to UHD conversion was met, which resulted in a binary map showing whether a LDR pixel is projected be developed or not. For each block having LDR in 2016, the maximum proportion of conversion to UHD was set as the 75 percentiles of the observed 2001-2016 rate of all LDR blocks with LDR-to-UHD conversion within the county. This spatial allocation of LDR-to-UHD conversion was constrained to the 2016 LDR extent.

A similar approach was used to allocate non-LDR-to-UHD conversion, but the projection was conducted within the 2016 non-LDR extent. The two binary projections (i.e., LDR-to-UHD and non-LDR-to-UHD) were then combined to generate a complete map of UHD projection.

2.5.2. Allocation of LDR development

To be consistent with the 2001 and 2016 FUT layers, LDR projections were conducted at the U.S. Census block level. After allocating UHD locations, we calculated block-level LDR probabilities as the median value of UHD suitability of remaining undeveloped and available land within census blocks. That is, we excluded existing UHD, LDR, restriction areas, and projected UHD and then calculated the suitability for remaining block area to identify the location's likelihood for LDR growth. Finally, we implemented a probability layer-based thresholding method to predict specific locations where LDR development are most likely to occur in 2040. Like UHD projections, the thresholding method tested a series of thresholds per county until the LDR demand was met, with the amount of residual demand allocated to most probable remaining block. All county-wide projections were finally mosaiced to a nationwide map.

3. Model validation

We first evaluated our projected UHD and LDR maps through discussions and visual evaluation, including by AFT's regional experts across the country. In particular, we visually assessed the location, size, and pattern of projected urban clusters based on high-resolution aerial photography, thematic land use maps, and knowledge of local to regional urban environments. While this visual assessment was able to inform our understanding of the reliability and robustness of our models and projections, quantitative evaluation of the 2040 BAU projections and other scenario models was not possible due to lack of (future) reference data.

Thus, to also quantitatively evaluate our BAU model performance, we compared projected urban development with actual growth for the period 2001 to 2016. Using 2001 as the baseline year and observed change from 2001-2016 for demand, we first ran the BAU scenario to estimate the locations of UHD and LDR growth between 2001 and 2016. This projected 2001-2016 urban growth based upon our developed model was then compared with reference urban growth observed by FUT 2001 and 2016 layers.

Ten cities/metropolitans were selected across the country to conduct pixel-wise site-specific locational accuracy assessment (Figure 5). They were selected to represent diverse biophysical and socioeconomic conditions of cities across the country and to target locations where AFT and CSP researchers are familiar. For each city/metropolitan area, we randomly selected 1000 30-m locations (500 each for change and non-change categories) and calculated accuracy metrics of overall accuracy (OA) and F1 score (Powers 2020). The stable UHD extent was removed from the non-change class, as UHD remains unchanged after being built and including it in the assessment would artificially increase the apparent reliability of our models.

$$OA = \frac{The\ number\ of\ correct\ classification}{Total\ number} \quad (3)$$

$$F1 = \frac{2*UA*PA}{UA+PA} \quad (4)$$

where UA and PA refer to User's Accuracy and Producer's Accuracy of the UHD/LDR class, respectively.

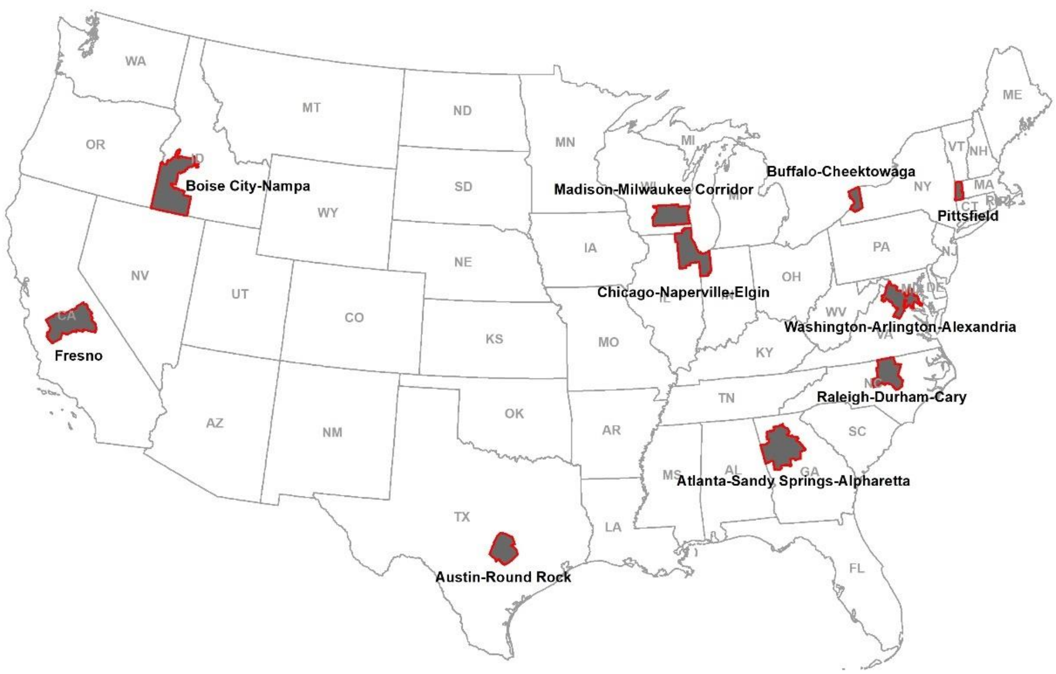

Figure 5. Distribution of 10 selected cities/metropolitans for accuracy assessment.

4. Results and discussion

4.1. Evaluation of BAU models

Running our models for the year 2016 results in similar patterns of urban development as compared with FUT-derived reference maps (Figure 6). Quantitatively, our modeling framework can predict UHD growth with reasonable overall accuracy of 67.1% and F1 score of 0.51 (Table 3). In general, the accuracies of UHD projection vary across cities/metropolises. The highest accuracies are achieved for Boise City-Nampa, Washington-Arlington-Alexandria, Austin-

Round Rock, and Chicago-Naperville-Elgin regions, with accuracies upwards of 70% and F1 scores close to or higher than 0.6. In contrast, accuracies are the lowest for Pittsfield and Buffalo-Cheektowaga areas (56-57%), with F1 scores only slightly above 0.2.

The estimation of LDR development is less reliable compared with UHD but still yields an overall accuracy over 60%. Given the variety of land use compositions within modeling regions, a high UHD estimation for a city/metropolitan area is not an assurance of high accuracy for its LDR projection. For example, Atlanta-Sandy Springs-Alpharetta has the highest LDR projection accuracy (F1 score of 0.57) but is middle-of-the-road for UHD projection accuracy. The lowest LDR accuracies were achieved in Fresno and the Madison-Milwaukee Corridor (F1 score of 0.12 and 0.25, respectively).

Note, however, these results reflect the accuracy of UHD and LDR *growth* instead of their total *extent*. Estimating growth (a dynamic land use class) is more difficult than estimating total extent (where most land is static) but gives a better indication of the model's performance in estimating agricultural land conversion, which is our output of interest. Given 1) the complexity of driving forces of urban development, 2) limited data availability for some variables needed to predict UHD and LDR (e.g., farm size), and 3) inherent uncertainty in making future predictions (Liu et al. 2017; Sohl et al. 2017), the achieved accuracies should be considered both sufficient and appropriate for making future projections to inform land conservation and prioritization. For reference, commonly acceptable accuracies for the historic *detection* of dynamic, remotely sensed land cover change classes are often between 60 to 70%. Thus, achieving a similar level of overall accuracy for the *prediction* of change should meet or exceed performance requirements for most applications of this data.

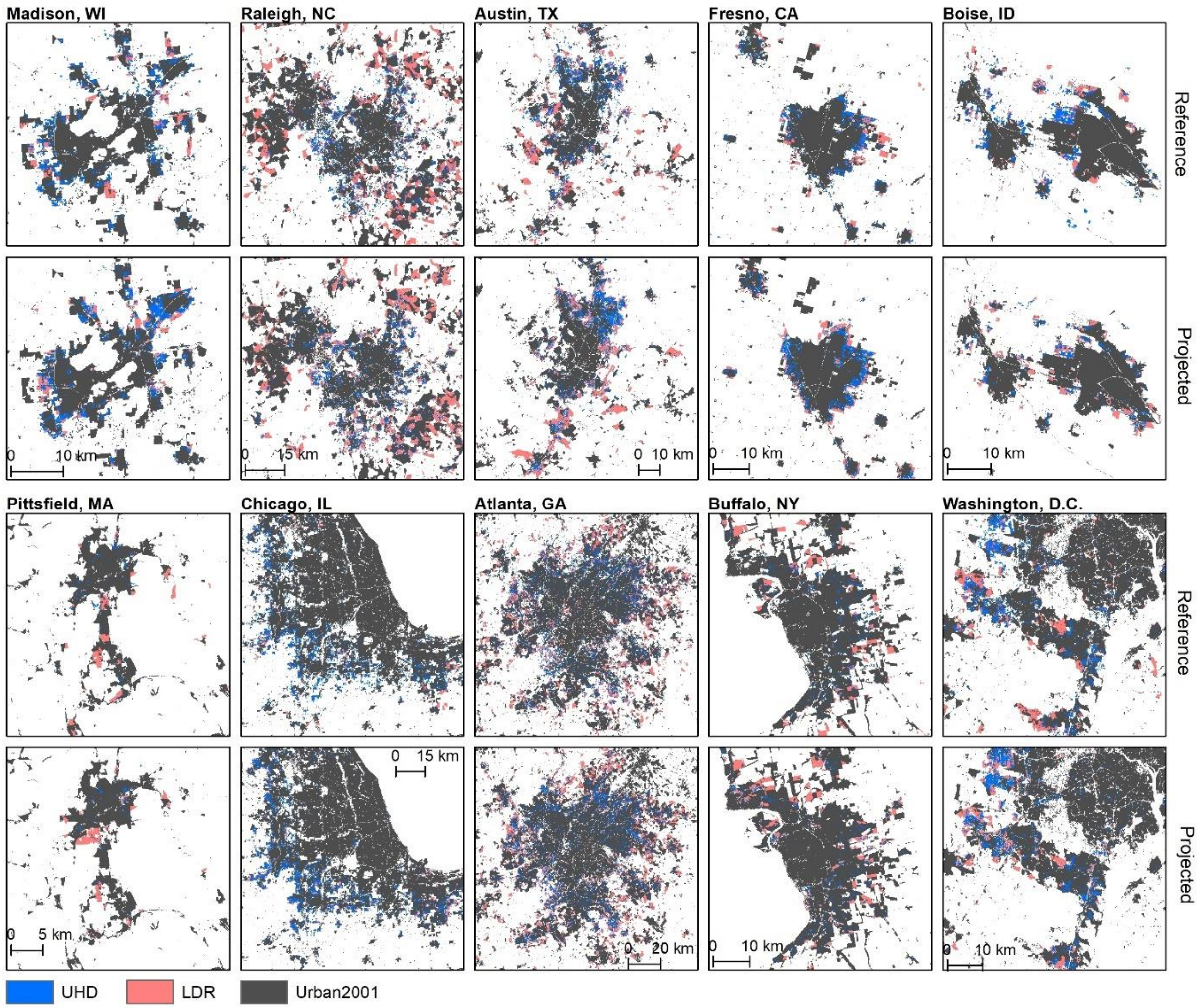

Figure 6. Comparison of projected and actual growth of urban and highly developed (UHD) and low-density residential (LDR) between 2001 and 2016 for 10 select cities/metropolitans.

Table 3. Accuracy assessment of projected UHD growth from 2001 to 2016 compared to actual changes.

	UHD		LDR	
Cities/metropolitans	**OA (%)**	**F1 score**	**OA (%)**	**F1 score**
Madison-Milwaukee Corridor, WI	66.6	0.51	56.8	0.25
Raleigh-Durham-Cary, NC	68.5	0.55	65.3	0.50
Austin-Round Rock, TX	70.3	0.59	58.4	0.34
Fresno, CA	67.3	0.52	52.9	0.12
Boise City-Nampa, ID	76.0	0.68	59.3	0.32
Pittsfield, MA	56.2	0.22	61.9	0.40
Chicago-Naperville-Elgin, IL-IN-WI	70.1	0.59	57.7	0.30
Atlanta-Sandy Springs-Alpharetta, GA	66.0	0.52	67.5	0.57
Buffalo-Cheektowaga, NY	57.0	0.26	63.4	0.45
Washington-Arlington-Alexandria, DC-VA-MD-WV	72.6	0.63	62.0	0.43
Average	**67.1**	**0.51**	**60.5**	**0.37**

4.2. Spatial patterns of BAU projections

The projected 2040 BAU UHD and LDR development in Figure 7 shows that our proposed model provides reasonable urbanization patterns. Our maps show that future urban development will occur in suburban to peri-urban areas where developable lands are available and close to existing low- to high-density built-up areas and transportation networks.

Our BAU projections see diverse local to nationwide urban growth by 2040. If urban development continues at the same pace as that in 2001-2016, our modeling shows additional 9.5 million acres of UHD development, with 6.2 million occurring on agriculutral land nationwide. Notable UHD increases are projected to occur especially in the Southeast, Texas, and California (Figure 8a). Despite their already being highly urbanized, several metropolitan areas in these states would continue to expand such as Riverside-San Bernardino-Ontario, CA, Dallas-Fort Worth-Arlington, Houston-The Woodlands-Sugar Land, and Austin-Round Rock-Georgetown of TX, Orlando-Kissimmee-Sanford, FL, Atlanta-Sandy Springs-Alpharetta, GA, and Raleigh-Cary, NC.

Arizona, Illinois, Tennessee, and South Carolina will also see increases of 250-350 thousand acres. Metropolitan areas like Pheonix-Mesa-Chandler, AZ, Chicago, IL, Nashville, TN, and Greenville, TN will experience the largest UHD gains in these states. In addition, we find several cities/metropolitan areas with sizeable UHD expansion in the Midwest and Eastern US, including Minneapolis-St. Paul-Bloomington, MN-WI, Milwaukee-Waukesha, WI, Columbus, OH, and Washington-Arlington-Alexandria, DC-VA-MD-WV. With the exceptions of California and Arizona, most other western states show relatively small UHD increases, ranging from <50 to 250 thousand acres.

Accompanying the high-density urban development, our BAU projections also show an additional 21.1 million acres of land that will be converted to LDR use. Compared to UHD, LDR projections show a higher contrast between the Western and Eastern US (Figure 8b). Texas and North Carolina show the most LDR development, with increases of >1.5 million acres, followed by Georgia, Tennessee, and Virginia of 0.9-1.5 million acres, and the Midwest (Minnesota, Wisconsin, Michigan, and Missouri) and some Southeast states (South Carolina, Alabama, Mississippi, and Florida) of 0.3-0.9 million acres.

Lastly, as climate change continues, it will likely affect the patterns of land use change we project here. For example, sea-level rise may displace a portion of current populations and developed land, resulting in altered development patterns. In the online data associated with this report, maps of locations likely to be affected by climate-induced sea-level rise by the year 2040 are available to overlay with the projected UHD and LDR development layers to help initially assess and visualize these interactions. Further information on such projected climate impacts, including the methods used to project sea-level rise, are detailed in the accompanying report entitled "Description of the approach, data and analytical methods used for the Farms Under Threat 2040 projections of climate-related crop and land-use suitability, and sea-level rise."

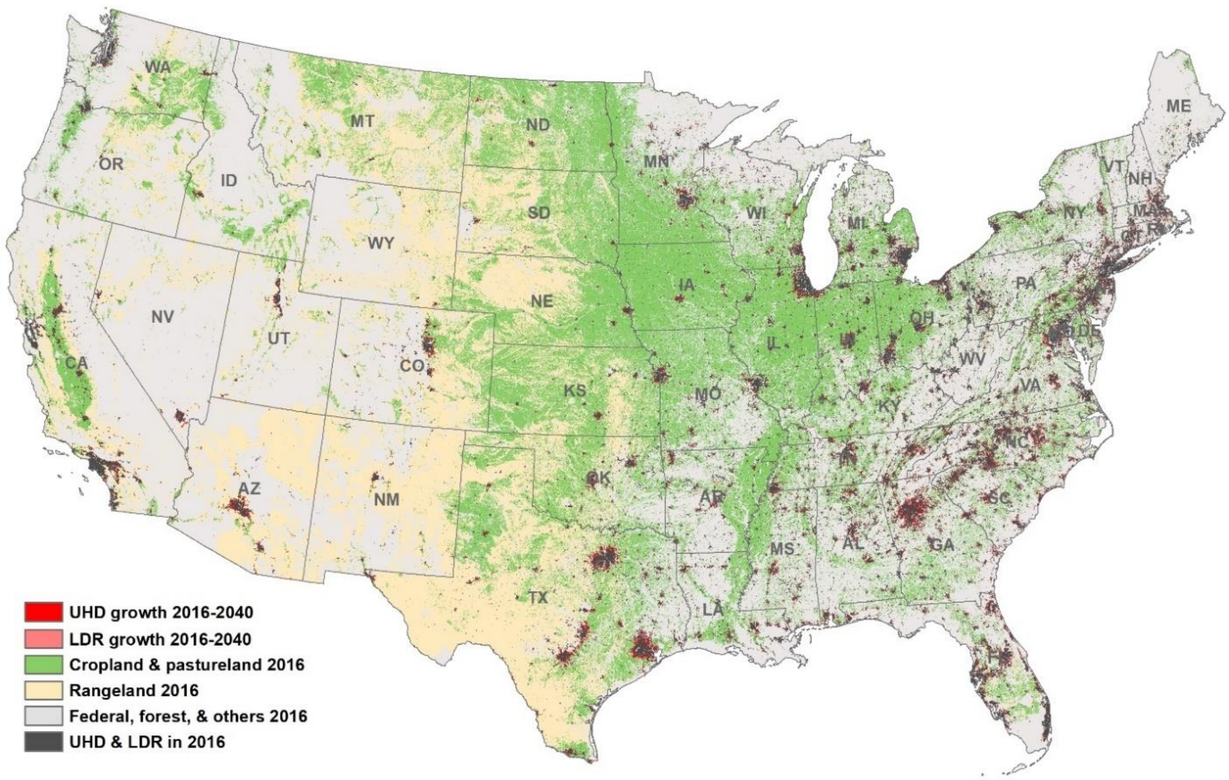

Figure 7. Projected urban and highly developed (UHD) and low-density residential (LDR) growth by 2040 under the Business-as-Usual scenario.

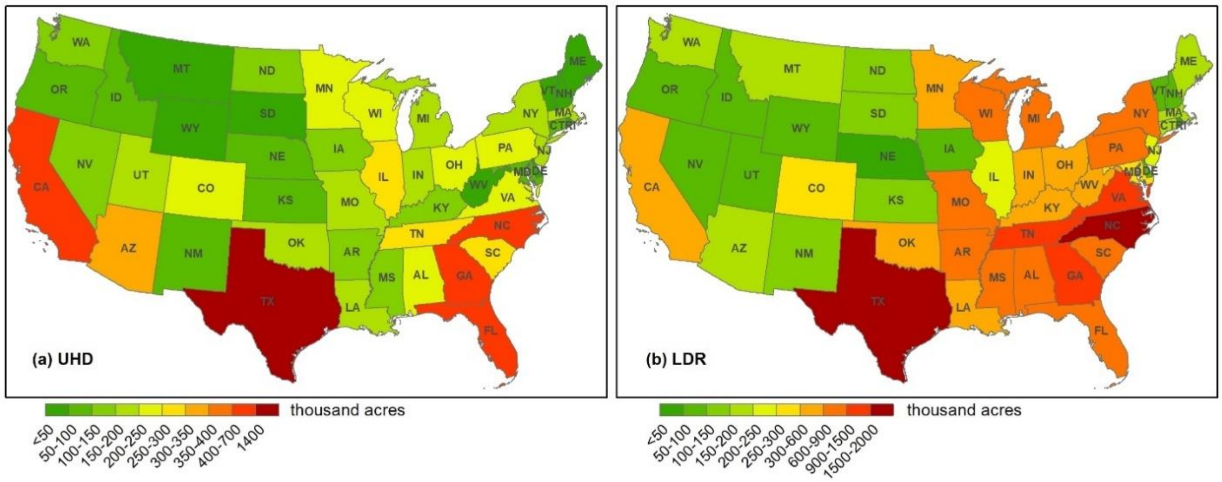

Figure 8. Projected per state (a) urban and highly developed (UHD) and (b) low-density residential (LDR) growth by 2040 under the Business-as-Usual scenario.

References

Breiman, L., 2001. Random forests. *Machine learning*, *45*, 5-32.

Chen, G., Li, X., Liu, X., Chen, Y., Liang, X., Leng, J., Xu, X., Liao, W., Qiu, Y., Wu, Q., Huang, K., 2020. Global projections of future urban land expansion under shared socioeconomic pathways. *Nat Commun*, *11*, 537. doi: 10.1038/s41467-020-14386-x

Elvidge, C.D., Baugh, K.E., Kihn, E.A., Kroehl, H.W., Davis, E.R., Davis, C.W., 1997. Relation between satellite observed visible-near infrared emissions, population, economic activity and electric power consumption. *International Journal of Remote Sensing*, *18*, 1373-1379.

Freedgood, J., Hunter, M., Dempsey, J., Sorensen, A. (2020). Farms Under Threat: The State of the States. In. Washington, D.C.: American Farland Trust

Liu, X., Liang, X., Li, X., Xu, X., Ou, J., Chen, Y., Li, S., Wang, S., Pei, F., 2017. A future land use simulation model (FLUS) for simulating multiple land use scenarios by coupling human and natural effects. *Landscape and Urban Planning*, *168*, 94-116.

Nolte, C., 2020. High-resolution land value maps reveal underestimation of conservation costs in the United States. *Proc Natl Acad Sci U S A*, *117*, 29577-29583. doi: 10.1073/pnas.2012865117

Nowak, D.J., Crane, D.E., Stevens, J.C., Hoehn, R.E., Walton, J.T., Bond, J., 2008. A ground-based method of assessing urban forest structure and ecosystem services. *Aboriculture & Urban Forestry. 34 (6): 347-358.*, *34*.

Powers, D.M., 2020. Evaluation: from precision, recall and F-measure to ROC, informedness, markedness and correlation. *arXiv preprint arXiv:2010.16061*.

Seto, K.C., Guneralp, B., Hutyra, L.R., 2012. Global forecasts of urban expansion to 2030 and direct impacts on biodiversity and carbon pools. *Proc Natl Acad Sci U S A*, *109*, 16083-16088. doi: 10.1073/pnas.1211658109

Sohl, T., Dornbierer, J., Wika, S., Sayler, K., Quenzer, R., 2017. Parcels versus pixels: modeling agricultural land use across broad geographic regions using parcel-based field boundaries. *Journal of Land Use Science*, *12*, 197-217. doi: 10.1080/1747423x.2017.1340525

Sorensen, A., Freedgood, J., Dempsey, J., Theobald, D. (2018). Farms Under Threat: The State of America's Farmland. In. Washington, DC: American Farmland Trust

Sutton, P.C., Elvidge, C.D., Ghosh, T., 2007. Estimation of gross domestic product at sub-national scales using nighttime satellite imagery. *International Journal of Ecological Economics & Statistics*, *8*, 5-21.

Tyrväinen, L., Silvennoinen, H., Kolehmainen, O., 2003. Ecological and aesthetic values in urban forest management. *Urban Forestry & Urban Greening*, *1*, 135-149.

Xie, Y., Weng, Q., Fu, P., 2019. Temporal variations of artificial nighttime lights and their implications for urbanization in the conterminous United States, 2013–2017. *Remote Sensing of Environment*, *225*, 160-174. doi: 10.1016/j.rse.2019.03.008

Ziter, C.D., Pedersen, E.J., Kucharik, C.J., Turner, M.G., 2019. Scale-dependent interactions between tree canopy cover and impervious surfaces reduce daytime urban heat during summer. *Proceedings of the National Academy of Sciences*, *116*, 7575-7580.